IEICE Communications Express, Vol.13, No.9, 351–354

ComEX

LETTER

Two types of bandwidth evaluation of crossed spherical helix antennas using numerical simulation

Takuma Shimada[1, a)], **Mina Nishie**[2], **Keisuke Noguchi**[2], **Masato Odagaki**[1], **and Keisuke Fujita**[1, b)]

Abstract Comparing the bandwidths of a crossed spherical helix antenna (XSHA) and conventional antennas is challenging owing to significant change in the radiation efficiency with respect to frequency even at low voltage standing wave ratio (VSWR). Thus, two types of evaluation were performed in this work to demonstrate the wideband property of XSHA. First, the antennas were assumed to be made of a perfect conductor and were compared regarding only the VSWR bandwidth. Next, we compared the bandwidth at radiation efficiency of lossy antennas based on the generalized effective fractional bandwidth (B_e). B_e is the product of the bandwidth and the radiation efficiency varying with frequency. Numerical simulations were conducted to compare the bandwidths for $VSWR \leq 3$. The bandwidth of the XSHA is 2.19 and 2.11 times wider than those of single resonance antenna in lossless and lossy cases, respectively. Compared with a dual resonance antenna, the bandwidth of the XSHA is 1.36 times greater at acceptable radiation efficiencies of 50%.

Keywords: small antenna, spherical helix antenna, bandwidth enhancement, multimode excitation, crossed two-wire, radiation efficiency
Classification: Antennas and propagation

1. Introduction

In recent years, research has been conducted to enhance the bandwidth of small antennas. Antennas for portable devices should be small in size to facilitate portability and reduce cost. However, downsizing the antenna results in a narrow bandwidth [1]. To improve the speed and quality of mobile wireless communication systems, methods have been developed to improve the bandwidth of small antennas.

Two methods exist for enhancing the bandwidth of a small antenna: One involves minimizing the Q factor of single resonance radiating element, and the other achieves dual resonance with addition of a matching structure such as a folded dipole-like structure. To minimize the Q factor, a method of arranging radiating elements on a spherical surface is being researched based on current distribution analysis using spherical wave expansion. Whereas, to utilize dual resonance, a method of multi-mode excitation has been proposed to excite both the radiation and transmission line modes [2].

[1] Faculty of Engineering, Maebashi Institute of Technology, 460–1 Kamisadorimachi, Maebashi-shi, Gumma-ken 371–0816, Japan
[2] College of Engineering, Kanazawa Institute of Technology, 7–1 Ohgigaoka, Nonoichi-shi, Ishikawa-ken 921–8501, Japan
[a)] m2256011@maebashi-it.ac.jp
[b)] fujita@maebashi-it.ac.jp

DOI: 10.23919/comex.2024XBL0038
Received March 3, 2024
Accepted April 16, 2024
Publicized June 11, 2024
Copyedited September 1, 2024

A study combining these two methods has also been introduced [3]. Specifically, an antenna was developed that expands the bandwidth by providing dual resonance to a spherical helix antenna with a low Q factor using a transmission line. This antenna has a considerably wider bandwidth than a one-arm conventional spherical helix antenna. However, a transmission line exhibits large loss owing to current cancelation and rapid variation of radiation efficiency with the frequency.

To avoid the large change in radiation efficiency caused by the cancellation of current in a transmission line, we propose a crossed spherical helix antenna (XSHA) [4]. This antenna comprises two spherical helix wires with opposite winding directions positioned on the inner and outer spherical surfaces. Moreover, XSHA decreases the cancellation of radiating current, thereby resulting in enhanced stability in radiation efficiency across the operating frequency range. By arranging the lengths of two elements to resonate at slightly different frequencies, both wide bandwidth for radiation efficiency and low VSWR can be achieved. However, no comparison has been made between the bandwidth of this antenna and that of a conventional antenna.

Metrics that reflect the frequency variation of the radiation efficiency should be used to ensure a fair evaluation of the bandwidth of the antenna. It is difficult to compare the bandwidth because conventional metrics, such as the Q factor, assume constant radiation efficiency over the operating frequency. However, multiple resonances can cause significant variations in radiation efficiency with respect to frequency, making the conventional Q factor unsuitable for comparing these cases. Thus, two methods for comparing the bandwidth of multiple resonant antennas are presented. One method assumes lossless materials. The other method involves comparing using a metric of generalized effective bandwidth.

Comparing the bandwidth using multiple methods from different perspectives is more appropriate than applying only one method. Moreover, it is more effective to evaluate the potential upper bound of the bandwidth determined from the geometric structure of an antenna under lossless conditions. The effective bandwidth is regarded as the modified version of the conventional bandwidth. The method effectively considers the frequency-dependent radiation efficiency owing to the lossy material. These two methods (lossless and lossy) can separately evaluate the effect of components on the bandwidth of both the geometric structure and the material property.

In this study, we assess the bandwidth of XSHA based

on numerical simulation results using two types of evaluations. First, we compare the numerical results for the lossless cases. We evaluate the bandwidth that is the potential upper bound of bandwidth determined from the geometric structure. Subsequently, the normalized effective bandwidth that considers a significant variation in the radiation efficiency of XSHA and bandwidth of conventional antennas are compared. Consequently, we compare the bandwidths of multiple antennas with different frequency characteristics of radiation efficiency. Finally, a summary and future challenges are discussed.

2. XSHA and antennas used for comparison

Figure 1(a) presents a schematic view of the XSHA [4] and coordinate axis. The XSHA is a combination of two spherical helix antennas that are placed on the surfaces of two concentric spheres. The conductors placed on the outer and inner surfaces of the spheres are referred to as SHA-out and an SHA-in, respectively. The feed point is located at the center of the entire length of the SHA-out. The wires of SHA-out and SHA-in are designed with a reverse wound shape to prevent the cancellation of the radiated field. The arrangement of the spherical helix antennas as radiating elements can be expressed using the spherical coordinate system (r, θ, φ). When the distance from the center point of the sphere to the surface where SHA-out and SHA-in exist is $r = r_{\text{out}}, r_{\text{in}}$, a shape of wires can be represented as follows:

$$\theta = 2\arctan e^{\gamma\varphi}, \gamma = \gamma_{\text{out,in}} \tag{1}$$

$$\gamma = \frac{I_\theta}{I_\varphi} \tag{2}$$

where I_θ and I_φ are the θ and φ components of the current I on the each radiating element, respectively. Both SHA-out and SHA-in have a shape parameter of $\gamma_{\text{out,in}}$, which represents the winding shape of a wire. The wire length of each radiating element can be written as:

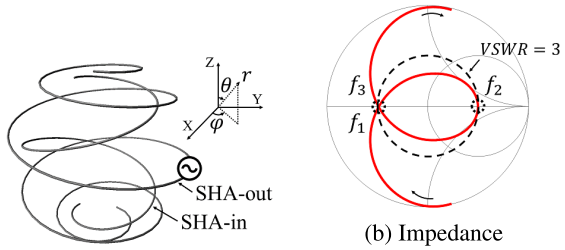

(a) XSHA

(b) Impedance characteristics of a dual resonance antenna in Smith chart

Fig. 1 Simulation model of XSHA and impedance characteristics of a dual resonance antenna

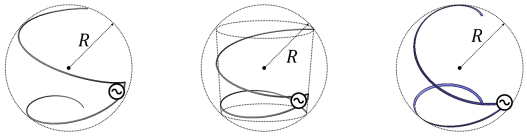

(a) SHA (b) NHA (c) FSHA

Fig. 2 Linearly polarized antennas selected for a bandwidth comparison

$$l_{\text{out,in}} = \left(\frac{\pi}{2} - \theta_c\right) \cdot \left(2r_{\text{out,in}}\sqrt{1 + \gamma_{\text{out,in}}^{-2}}\right) \tag{3}$$

where θ_c is the cut-off zenith angle, which determines the top and bottom end of a spherical helix antenna. The SHA-out is positioned for 180° rotation around the z-axis with respect to the SHA-in and wound in the opposite direction. The reverse winding results in the opposite signs of γ_{out} and γ_{in}. The spherical helix antennas can be resonated by selecting a length of $l_{\text{out,in}} \approx \lambda/2$, where λ represents the wavelength of the operating frequency. In addition, fine adjustment of θ_c enables the control of the resonance frequency.

Figure 1(b) depicts the one representative result of the impedance characteristics for an antenna with dual resonance, such as XSHA. Three resonance frequencies of $f_{1,2,3}$ indicate a dual resonance resulting from a combination of series and parallel resonances. The selection of the appropriate resonance frequency can increase the bandwidth of the VSWR of the dual resonances compared to the case of a single resonance.

Figures 2(a)–(c) display schematic views of antennas competing with XSHA. Antennas are designed within a sphere with a radius of $r = R = r_{\text{out}}$. Figure 2(a) is a single-arm spherical helix antenna (SHA) [5] that exhibits a single resonance, low Q factor, and high radiation efficiency. Figure 2(b) is a normal mode helix antenna (NHA) [5] that has a circumference sphere with the same radius as that of XSHA. Figure 2(c) is a folded spherical helix antenna (FSHA) [3] that exhibits a dual resonance; a wideband and small antenna whose radiation efficiency varies rapidly with frequency. All θ_c values for the XSHA, SHA, and FSHA were designed as 20°. According to Fig. 1(b), the XSHA and FSHA have the largest bandwidth when $VSWR = 3$.

3. Comparison of bandwidth using numerical simulation

Numerical simulations were conducted to compare the bandwidths B of different frequency characteristics of the radiation efficiency η. The conventional $B\eta$ product is a an established method for comparing the bandwidths of single resonance antennas. However, the $B\eta$ product cannot handle the comparison between a double resonant antenna and a single resonant antenna. Therefore, the comparison of bandwidths using the two methods, lossless and lossy, is crucial because they can provide different aspects and more advantages.

3.1 Comparison of bandwidth with a perfect conductor

We assumed a wire made of a perfect conductor to eliminate the effects of frequency-dependent changes in radiation efficiency. Comparisons using simulations for each antenna were performed with antenna sizes $kR = 0.46$, where k is the wave number. Each antenna was designed to satisfy the criteria of an electrically small antenna ($kR < 0.5$) and to maximize bandwidth for $VSWR \leq 3$. Further, all antennas were designed to occupy the maximum possible space within a sphere of radius 15 mm. The radiating element of each antenna comprised a wire with $a = 0.15$ mm. For XSHA, as $r_{\text{out}} = 15.0$ mm, $r_{\text{in}} = 12.7$ mm, $\gamma_{\text{out}} = 0.125$, and $\gamma_{\text{in}} = -0.268$. In addition, the XSHA and SHA were

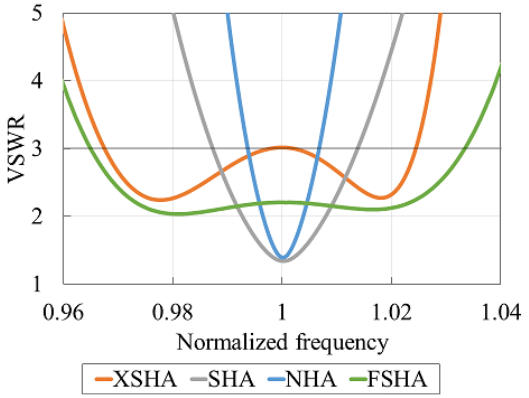

Fig. 3 VSWR results for the XSHA, SHA, NHA, and FSHA antennas obtained via simulation using a perfect conductor at antenna size of kR = 0.46

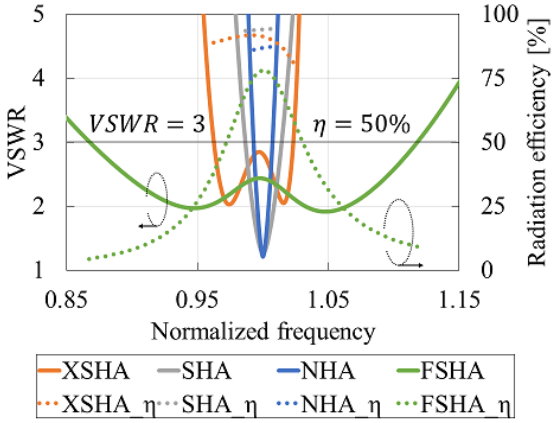

Fig. 4 VSWR and radiation efficiency results for the XSHA, SHA, NHA, and FSHA obtained via simulation using copper with conductivity of 5.98× 10^7 S/m at electrical size of kR = 0.46

designed with θ_c = 20°. FSHA under lossless conditions was also designed in comparison with the radiation characteristics. The parameters of FSHA, including the relative permittivity of the substrate, were adjusted to avoid the mismatch owing to the vanishing of the loss resistance. Consequently, the impedance can be matched to achieve wideband characteristics under lossless conditions.

Figure 3 shows the bandwidth of each antenna when $VSWR \leq 3$ and antenna size kR = 0.46. Bandwidths of XSHA, SHA, NHA, and FSHA are indicated by orange, gray, blue, and green lines, respectively. The relative bandwidths of XSHA, SHA, NHA, and FSHA are 5.71%, 2.61%, 1.30%, and 6.13%, respectively. The results indicate that FSHA has the broadest bandwidth characteristics among the antennas, followed by XSHA, when the effect of material is omitted.

3.2 Comparison of bandwidths considering variations in radiation efficiency with respective to frequency

A metric that can consider the variation of radiation efficiency with frequency was calculated to compare the bandwidth of each antenna. The generalized effective fractional bandwidth (B_e) [3] was proposed as a generalization of the product of bandwidth and radiation efficiency ($B\eta$) and is expressed as

$$B_e = \int_{f_{\text{low}}}^{f_{\text{high}}} \eta(f) df \tag{4}$$

where the upper and lower values of normalized frequency for $VSWR \leq 3$ and $\eta \geq 50\%$ are denoted as f_{high} and f_{low}, respectively. The metric B_e is equivalent to $B\eta$ when the radiation efficiency is constant over operating frequency range. Further, the frequency f is regarded as normalized by the central resonance frequency f_2.

The antennas were compared for antenna size kR = 0.46. The design conditions for each antenna were the same as those explained in Sec. 3.1. The conductivity for the copper material was set to 5.98×10^7 S/m.

Figure 4 shows the VSWR and radiation efficiency at kR = 0.46. The horizontal axes for SHA and NHA were normalized using the resonance frequency; whereas, those of XSHA and FSHA were normalized using the center frequency of f_2. Radiation efficiency is shown as a dashed line only when $VSWR \leq 3$, while other VSWR values are indicated with dotted lines. The orange, gray, blue, and green lines indicate the XSHA, SHA, NHA, and FSHA, respectively. Let $\Delta\eta$ be the difference between the maximum and minimum radiation efficiency in a range from f_{low} to f_{high}. The $\Delta\eta$ values for the XSHA, SHA, NHA, and FSHA were 10.9, 0.70, 1.23, and 27.6 points, respectively, and $\Delta\eta$ for the XSHA was found to be larger than those of the SHA and NHA and smaller than the FSHA. The single and dual resonance antennas showed significant differences in $\Delta\eta$.

The radiation efficiencies of single and dual resonance antennas with different frequency-dependent characteristics can be compared using B_e. B_e was calculated from the simulation results for each antenna using Eq. (4). B_e for the XSHA, SHA, NHA, and FSHA were 5.45, 2.58, 1.25, and 4.01, respectively. The B_e values of the XSHA were 2.11, 4.36, and 1.36 times higher than those of the other antennas, respectively. After considering the variation of radiation efficiency with frequency, the dual resonance antenna has wider bandwidth characteristics than the single resonance antenna. Additionally, the XSHA exhibited larger bandwidth than the FSHA at $VSWR \leq 3$ and $\eta \geq 50\%$.

4. Conclusion

We validated the broadband property of the XSHA via numerical simulations considering two aspects. Assuming a perfect conductor to eliminate ohmic losses, the XSHA (dual resonance antenna) exhibited a bandwidth 2.19 times greater than that of conventional SHA (single resonance antenna). The results of the bandwidth comparison under lossless conditions indicate that XSHA cannot exceed the bandwidth of FSHA. The comparison under lossless conditions suggests that FSHA exhibits the greatest potential for bandwidth if the power dissipated in the material could be drastically improved. Numerical simulations with imperfect conductors indicate that the difference between the maximum and minimum radiation efficiencies ($\Delta\eta$) for the XSHA is smaller than that of the FSHA (double resonant antenna). Considering B_e, the XSHA presents a bandwidth that is 1.36 times wider than that of the FSHA. From a practical perspective, the comparison of B_e reveals that XSHA can achieve

a large bandwidth. The result can be attributed to its simple structure compared to FSHA without a lossy dielectric substrate. Both lossless and lossy simulation results confirm that the wide bandwidth of XSHA can be explained by different perspectives of its geometrical structure and the material properties.

A future challenge will be to consider matching methods that can overcome an extremely low input impedance owing to miniaturization. Accordingly, we will consider methods that can manage both a wide bandwidth of the radiation efficiency and VSWR.

Acknowledgments

This work was supported by JSPS KAKENHI Grant Number 21K14158.

References

[1] C.A. Balanis, *Antenna Theory: Analysis and Design*, Wiley, 2016.
[2] K. Noguchi, "Bandwidth enhancement of small and planar antennas using multi–mode excitation," *IEICE Trans. Commun.*, vol. 99, no. 9, pp. 655–664, Sept. 2016.
[3] T. Shimada, M. Nishie, K. Noguchi, M. Odagaki, and K. Fujita, "Bandwidth enhancement of a spherical helix antenna with multi-mode excitation," to be published in *IEICE Trans. Commun.* (Japanese Edition), vol. J106-B, no. 11, Nov. 2023.
[4] T. Shimada, M. Nishie, K. Noguchi, M. Odagaki, and K. Fujita, "A wideband small double-layer spherical helix antenna with crossed elements," accepted to *IEICE Trans. Commun.* (Japanese Edition).
[5] S.R. Best, "Electrically small resonant planar antennas: optimizing the quality factor and bandwidth," *IEEE Antennas Propag. Mag.*, vol. 57, no. 3, pp. 38–47, June 2015. DOI: 10.1109/map.2015.2437271